of light wavelength. Conversely, the fact that gels are clear in decalin deserves to be commented. As the scattering is proportional to Δn^2, gels from decalin scatter and absorb 2.5–3 times less than gels from the other solvents ($\Delta n \simeq 0.11$ in decalin and $\Delta n \simeq 0.16$–0.17 in the other solvents). Scattering from decalin gels, if weak, exists and is offhand comparable to that of agarose gels in water for which experiments have shown it to be consistent with the presence of large structures.[10] From this we conclude that transparency is far from being a well-grounded criterion to anticipate on the gel structure at the molecular level. Only careful light scattering experiments can be decisive.

Conclusion

In this paper, both thermodynamic properties and morphology of iPS gels have been investigated. We have shown that when the gels are prepared through phase separation prior to crystallization, a turbid–clear transition is observed the temperature at which it occurs is linked to the Θ-point. Accordingly, for solvents wherein the transition is well above 20 °C, the gel is turbid at room temperature. This phenomenon, which must not be confused with a crystallization, is thought to arise from a secondary phase separation undergone by the chains that failed to incorporate into the network during gelation.

In addition, we report the observation of a conformational transformation of the network from the 12_1 to the 3_1 helical form. This transformation is pointed out either by using very slow heating rates in DSC experiments or by annealing below the gel melting point (i.e., when still under the 12_1 form). This transition takes place together with the rising of opaqueness.

Finally, morphological investigations reveal that the iPS gels are of fiberlike nature which leads to the dismissal of the fringed-micelle model to describe the structure of such gels.

This study also enables one to discuss and elucidate the various origins of the gel visual aspect.

References and Notes

(1) Tokahashi, A. *Polym. J.* **1973**, *4* (4), 379.
(2) Lemstra, P. J.; Challa, G. *J. Polym. Sci., Polym. Phys. Ed.* **1975**, *13*, 1809.
(3) Girolamo, M.; Keller, A.; Miyasaka, K.; Overbergh, N. *J. Polym. Sci., Polym. Phys. Ed.* **1976**, *14*, 39.
(4) Overbergh, N.; Berghmans, H. *Polymer* **1977**, *18*, 883.
(5) Berghmans, H.; Govaerts, F.; Overbergh, N. *J. Polym. Sci., Polym. Phys. Ed.* **1979**, *17*, 1251.
(6) Wellinghoff, S.; Shaw, J.; Baer, E. *Macromolecules* **1979**, *12*, 932.
(7) Yang, Y. C.; Geil, P. H. *J. Macromol. Sci., Phys.* **1983**, *B22* (3), 463.
(8) Sundararajan, P. R.; Tyrer, N. J.; Bluhm, T. L. *Macromolecules* **1982**, *15*, 286.
(9) Eldridge, J. E.; Ferry, J. D. *J. Phys. Chem.* **1954**, *58*, 992.
(10) Feke, G. T.; Prins, W. *Macromolecules* **1974**, *7*, 527.
(11) Sundararajan, P. R.; Tyrer, N. *Macromolecules* **1982**, *15*, 1004.
(12) Sundararajan, P. R. *Macromolecules* **1979**, *12*, 575.
(13) Magre, E. P.; Boon, J. "2nd Microsymposium on the Structure of Organic Solids"; Prague, 1968.
(14) Kusuyama, H.; Takase, M.; Higashihata, Y.; Tseng, H. T.; Chatani, Y.; Tadokoro, H. *Polymer* **1982**, *23*, 1256.
(15) Helms, J. B.; Challa, G. *J. Polym. Sci., Part A-2* **1972**, *10*, 1447.
(16) Guenet, J. M.; Gallot, Z.; Picot, C.; Benoit, H. *J. Appl. Polym. Sci.* **1977**, *21*, 2181.
(17) Lemstra, P. J.; Kooistra, T.; Challa, G. *J. Polym. Sci., Part A-2* **1972**, *10*, 823.
(18) Talen, J. L.; Challa, G. *J. Polym. Sci., Polym. Lett. Ed.* **1966**, *4*, 407.
(19) Cahn, J. W. *J. Am. Ceram. Soc.* **1969**, *52*, 118.
(20) Kirgbaum, W. R.; Woods, J. D. *J. Polym. Sci., Part A-2* **1964**, 3075. Krigbaum, W. R.; Kurz, J. E.; Smith, P. *J. Phys. Chem.* **1961**, *65*, 1984.
(21) Stamhuis, J. E.; Pennings, A. J. *Br. Polym. J.* **1978**, *10*, 221.
(22) Tohyama, K.; Miller, W. G. *Nature (London)* **1981**, *289*, 813.

Concerning Gelation Effects in Atactic Polystyrene Solutions

Raymond F. Boyer,† Eric Baer,‡ and Anne Hiltner*‡

Michigan Molecular Institute, Midland, Michigan 48640, and Department of Macromolecular Science, Case Western Reserve University, Cleveland, Ohio 44106.

Received February 7, 1984

ABSTRACT: Published data on gelation of atactic PS's as a function of $\bar{M}_w$ and concentration, C, in ten organic diluents with solubility parameters, $\delta_s^{1/2}$, from 7.8 to 10 have been reexamined in terms of entanglement effects, influence of $\delta_s^{1/2}$, and comparison with previously unexplored literature results on other PS–diluent systems. Three regions of gel behavior can now be defined: I, low $\bar{M}_w$, low C, no gels; II, intermediate combinations of C and $\bar{M}_w$ which lead to coil overlap, gels; III, high C and $\bar{M}_w$ giving both overlap and entanglements, supergels. T_{gel} (°C) at fixed C and $\bar{M}_w$ is strongly dependent on $\delta_s^{1/2}$, being a minimum when $\delta_s^{1/2} = \delta_p^{1/2}$. It has been demonstrated that $T_{gel} > T_g$ and that T_{gel} should not be identified with T_g except at $C < 50$–100 g/L. The sharp, thermally reversible melting of atactic PS gels at T_{gel} can be considered as a "local melting" of segment–segment contacts first postulated by Lobanov and Frenkel to explain $T > T_g$ relaxations. T_{gel} should be a phenomenon general to all atactic polymers. For PS one can write the numerical identity valid for comparable values of C: T_{gel}, °C ($C \geq 130$ g/L) $\equiv T_f > T_g$ (T_f being the "fusion-flow" temperature of Ueberreiter; $\equiv T_{ll} > T_g$ of Gillham and co-workers). The designation "T_{gel}" appears very appropriate for gelation phenomena of the type being discussed and should be retained.

Introduction

Gelation phenomena in solutions of isotactic PS at concentrations greater than 3–5% have been discussed in detail by Girolamo et al.[1] A number of perplexing results not germane to the present study were reported. However, the closing paragraphs discuss pertinent observations about interactions between isotactic and atactic PS's present in a common solvent. Each polymer species seems aware of and reacts to the presence of the other in a manner not then understood. The authors concluded[1] that these exploratory results are likely to have a bearing on the structure and properties of amorphous PS. This prediction

† Michigan Molecular Institute.
‡ Case Western Reserve University.

0024-9297/85/2218-0427$01.50/0

Table I
T_{gel} (°C) Dependence on $\bar{M}_w$ and Concentration[a]

$\bar{M}_w$	entanglement concn,[b] g/L	concn, g/L				
		30	70	100	140	180
4×10^3					−41	−23
2×10^4				−58	−33	−19
3×10^4			−68	−41	−25	−14
3.7×10^4 [c]			−54	−39	−27	−18
2×10^5	175	−53	−32	−28	−22	−14
4.1×10^5	85	−41	−26	−22	−16	−9
6.7×10^5	52	−32	−16	−9	−3	15[d]
2×10^6	17.5	−28	−12	−3	7.5	15[d]

[a] Estimated from Figure 4 of ref 3 except where noted. [b] Polymer–diluent systems are entangled at this concentration and all higher concentrations. [c] Concentrations changed to g/L from volume percent. Data from ref 2. [d] From short extrapolation of both straight lines at top of Figure 4 of ref 3.

seems to have been verified by subsequent publications in this series.

For example, Wellinghoff et al.[2] studied both isotactic and atactic PS gels formed by rapid quenching of solutions of the individual polymers. Of particular interest to the present investigation is their Figure 1 showing that atactic PS of $M = 37\,000$ forms gels in CS_2 over the concentration range 10–60 vol %. They also reported in the same figure melting points at 0.16 volume fraction for a series of molecular weights. It thus became clear that crystallinity was not necessary for the formation of PS gels.

A detailed investigation of a-PS gels as a function of $\bar{M}_w$, concentration, and solvent type was then pursued by Tan et al.,[3] which results form the subject matter of the present study. It was demonstrated in ref 3 that gels formed in a variety of diluents under those combinations of $\bar{M}_w$ and concentration for which overlap of polymer coils can occur. It was further demonstrated that reasonable enthalpies of activation were associated with the gelation process. No formal mechanism of gelation was proposed. One surprising feature noted in ref 3 was complete thermal reversibility of the gel temperature, in contrast to the case for gels from isotactic PS.

Our present purpose in reanalyzing these data was several-fold: (1) to establish an unambiguous distinction between T_{gel} and T_g phenomena, already suggested in ref 3; (2) to seek from the literature anything that helps to interpret T_{gel}, i.e., chain entanglements; (3) to correlate T_{gel} with solubility parameters of the solvents employed; (4) to compare these results with related data in the prior literature; and (5) to establish a mechanism to account for such sharp, thermally reversible gel formation and disappearance with a nonpolar atactic polymer in moderately concentrated solutions.

Entanglement Effects

Since the three PS's of lowest molecular weight, $\bar{M}_w = 4 \times 10^3$, 2×10^4, and 3×10^4, were all below the critical molecular weight for entanglement, $C_c = 35\,000$ for PS, and still formed gels, it was evident that entanglements were not required for the gelation mechanism. Instead, the overlap criterion developed in ref 3 appeared to be a necessary condition to form gels. Entanglement effects, if present, could at most modify gel temperatures and then only at the highest molecular weights, as we shall now demonstrate.

Values of T_{gel} as a function of $\bar{M}_w$ at constant concentration were estimated from an enlarged plot of Figure 4 in ref 3 with the results collected in Table I. Plots of T_{gel} vs. log $\bar{M}_w$ at these five fixed concentrations are shown in Figure 1. T_{gel} increases with $\bar{M}_w$, starts to level off in each case, and then exhibits a dramatic slope increase which starts at higher molecular weight as concentration decreases. The points for $\bar{M}_w = 6.7 \times 10^5$ are high for the top five curves, as if $\bar{M}_w$ were in error. This influenced our drawing of the lowest curve.

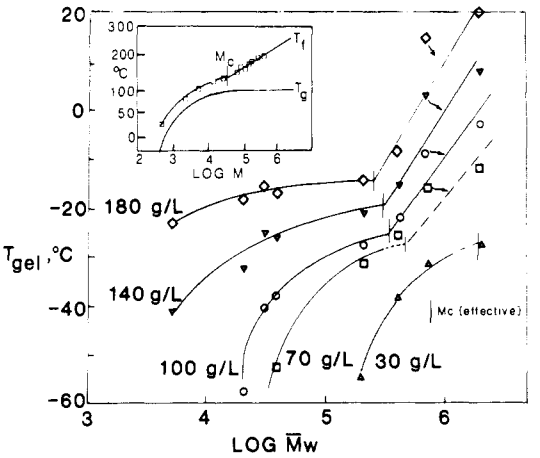

Figure 1. Plots of T_{gel} at the indicated concentrations in g/L of PS in CS_2 against log $\bar{M}_w$ of the narrow distribution PS's. T_{gel} values from Figure 4 of ref 3 and Figure 1 of ref 2. Short vertical bars are considered as effective entanglement molecular weights, M_c(eff). Inset shows T_f and T_g vs. log M data from Ueberreiter and Orthmann on pure PS.[4]

Such behavior appeared similar to that reported by Ueberreiter and Orthmann[4] for fractions of atactic PS and atactic PMMA.[4] They plotted a fusion-flow temperature, T_f ($T_f > T_g$), against log M and found that T_f increased at first with M, leveled off, and then experienced a sharp slope increase at M_c shown in the inset to Figure 1. T_g continued to level off with no change in character at M_c.

Since the slope change for pure polymer occurred exactly at M_c,[4] it was tempting to suggest that the slope change for each of the several curves in Figure 1 signified the effective entanglement molecular weight, M_c(eff), for that concentration of polymer.

Early work by Bueche on the viscosity of PS–diluent systems[5,6] and by Fox and Loshaek on several polymer systems[7] showed that M_c(eff) moved progressively to higher molecular weights on dilution according to

$$v_2 M_c(\text{eff}) = \text{constant} \quad (1)$$

where v_2 is the volume fraction of polymer and the constant for PS is 35 000.

Ferry[8] has reviewed the literature recently and concludes that eq 1 holds generally for nonpolar polymers such as PS although deviations may be found for polar polymers. He writes the general equation

$$M_c = M_c^{\circ} v_2^{-1} \quad (2)$$

where M_c is what we call M_c(eff) for the diluted polymer

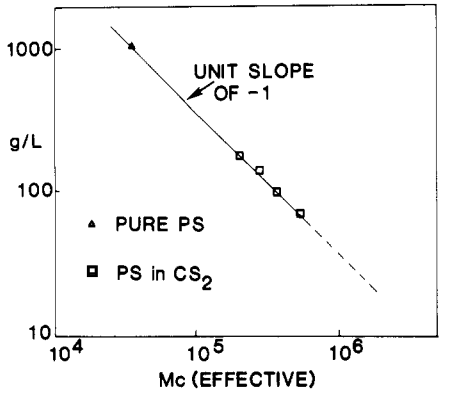

Figure 2. Plot of concentration in g/L against M_c(eff) from Figure 1, with an added point for pure PS at 1040 g/L. The linear plot, of slope −1, is consistent with eq 1 and 2.

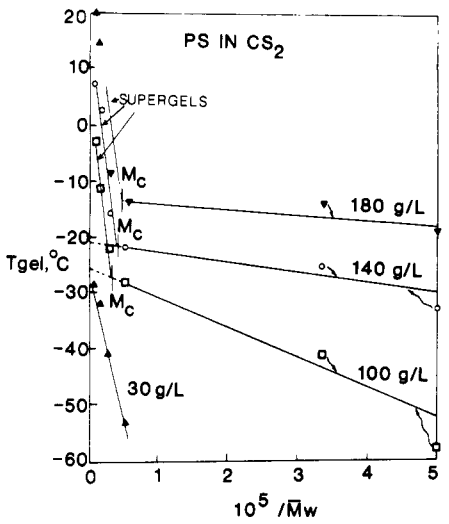

Figure 3. Plots of T_{gel}–$\bar{M}_w^{-1}$ at several concentrations of PS in CS_2 to dramatize the entanglement effect. The plots up to M_c are consistent with eq 4 behavior.

and $M_c°$ is the entanglement molecular weight for undiluted polymer.

Figure 2 is a log–log plot of concentration (g/L) against M_c(eff) in which we ignore the small difference between weight and volume fraction and employ the concentration units given in ref 3. Adding a point for pure PS leads to a reasonable fit with slope of −1, with the greatest uncertainty being at the two lowest concentrations of polymer.

Ueberreiter and Orthmann[4] noted that the curved portion of the T_f–log M plot below M_c could be linearized as

$$1/T_f = a + b \log M \tag{3}$$

where a and b are constants. It is simpler and more meaningful to use an alternate formulation for temperature–molecular weight effects, with symbols pertinent to our paper:

$$T_{gel} = T_{gel}(\infty) + K_{gel}\bar{M}_n^{-1} \tag{4}$$

where $T_{gel}(\infty)$ is the limiting value of T_{gel} at infinite molecular weight and K_{gel} is a constant. We neglect the small difference between $\bar{M}_n$ and $\bar{M}_w$.

Figure 3 is an eq 4 type plot based on selected isoconcentration data in Table I. Approximate linearity holds up to M_c(eff), suggesting that T_{gel} is influenced by end-group concentration below M_c but is then dominated by entanglements above M_c. The relative contributions above

Table II
Molecular Weight Dependence of T_{gel} at $M < M_c$[a]

concn of polymer, g/L	source of data	$-K_{gel} \times 10^{-4}$ [b]	$T_{gel}(\infty)$[b]	ref
30	T_{gel}–$\bar{M}_n^{-1}$	500	−26	this report
70	T_{gel}–$\bar{M}_n^{-1}$	258	−26	this report
100	T_{gel}–$\bar{M}_n^{-1}$	54	−26	this report
140	T_{gel}–$\bar{M}_n^{-1}$	18.6	−21	this report
180	T_{gel}–$\bar{M}_n^{-1}$	14	−13	this report
1040	T_f–$\bar{M}_n^{-1}$	13–21	142	this report[c]
1040	T_{ll}–$\bar{M}_n^{-1}$	15[d,e]	156[d,f]	9

[a] See Figure 3. [b] Based on eq 4. [c] Considerable error in estimating T_f and log M from published plot in ref 4. [d] Based on DSC and torsional braid analysis. [e] Called K_l in ref 9. [f] T_{ll} in ref 9.

M_c are evident on extrapolation of the linear portions to $\bar{M}_n^{-1} = 0$. The line for 30 g/L is in the unentangled region for all values of M except for 1.8×10^6.

Table II lists values of $T_{gel}(\infty)$ and K_{gel} for all five concentrations as well as $T_f(\infty)$ and K_f for pure PS from data in ref 4 and also quantities called K_l and $T_l(\infty)$ from ref 9. Implications of these collected results will be considered later in the present paper.

In Figure 3, as in Figure 1, it would be desirable to have data on other molecular weights below and above M_c to firm up the estimates of M_c(eff), $T_{gel}(\infty)$, and K_{gel}. Even so, there seems little doubt about the trends.

Figure 3 type plots were first employed by Stadnicki et al.[9] to demonstrate the dependence of a $T > T_g$ event on $\bar{M}_n$, to indicate the M value at which entanglements occur, and to show the effect of entanglements in increasing the $T > T_g$ temperatures.

Whereas ref 4 indicated no effect of M_c on T_g, more recent studies suggest that T_g does reflect a mild increase with entanglements, but nothing as great as that found for $T > T_g$. (See the comparison in Figure 6 of ref 9.) Turner[10] has also reported a mild entanglement effect on T_g for a variety of polymers.

Consideration of the results in Figures 1–3 leads to the conclusion that entanglements are having an influence in the sense of increasing T_{gel} and hence gel stability, so that higher melting points are observed than are predicted by the asymptotic limits of the curves from below to above M_c, as in Figure 3, and the $T_{gel}(\infty)$ values in Table II.

Moreover, since the shapes of the T_{gel}–log $\bar{M}_w$ curves in Figure 1 are similar to the T_f–log M plots shown in the inset to Figure 1, and not to the T_g plot, is appears correct to conclude that T_{gel} is not a T_g phenomenon but rather a $T > T_g$ event. This same conclusion was reached in ref 3 for PS in CS_2 based on known T_g values for PS and CS_2 and the T_g of CS_2. Other evidence to support this conclusion will be presented later.

Combining the overlap criterion of ref 3 with the entanglement effects of Figures 1–3 allows us to postulate three regimes of gelation behavior for atactic PS. These are shown schematically in Figure 4. CGC, the critial gelation concentration, is the lowest concentration at which a gel can be observed in CS_2 for the indicated $\bar{M}_w$. CGC values were plotted in Figure 9 of ref 3 and thereby related to the concentration at which overlap of polymer coils begins. The entanglement curve is based on Figure 2.

Experimental verification of Figure 4 is demonstrated by reading off from an enlargement of Figure 4 of ref 3 concentrations as a function of $\bar{M}_w$ for T_{gel} = constant. Numerical values are collected in Table III and plotted in Figure 5. Low-temperature gel isotherms, i.e., T_{gel} = −50 °C, tend to follow the CGC line whereas the T_{gel} = −10 °C isotherm is evidently dominated by entanglement effects at higher molecular weights.

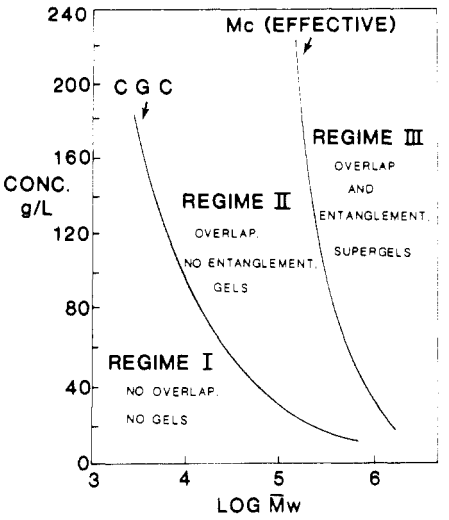

Figure 4. Schematic plot to define the three regimes of behavior shown by the T_{gel} data of ref 3. The lower line, labeled CGC, for critical gel concentration, demarks the start of coil overlap and is estimated from Figure 9 of ref 3. The entanglement line is based on Figure 2 of this report.

Table III
Concentrations in g/L for T_{gel} = constant[a]

	T_{gel}, °C				
$\bar{M}_w$	−10	−20	−30	−40	−50
4.0×10^3		190	160	145	129
2.0×10^4	220	174	142	126	111
3.0×10^4	200	157	124	104	91
3.7×10^4				105[b]	80[b]
2.9×10^5	200	145	82	51	33
4.1×10^5	175	111	53	34	20
6.7×10^5	95	42	32	20	12
2.0×10^6	85	31	22	12	5

[a] From Figure 4 of ref 3 except where noted. [b] From Figure 1 of ref 2.

We conclude that entanglements are not a necessary condition for gelation but do exert a modifying influence on T_{gel} values and other numerical aspects. For example, Figure 11 of ref 3 shows calculated enthalpies of activation for the gelation process as a function of log $\bar{M}_w$. We have redrawn this plot in Figure 6 to reflect the high likelihood that the onset of entanglement is responsible for the dramatic increase in ΔH observed in the original Figure 11 of ref 3. This is consistent with the stabilization of the gels by entanglement.

T_{gel} as an Isoviscous State

As mentioned, the T_f–log M curve in the inset of Figure 1 has been identified as an isoviscous state with $\eta \simeq 10^6$ P.[4] Since the T_{gel}–log M curves all have the same shape, it is tempting to speculate that they too represent an isoviscous state. We have not yet located viscosity data on solutions of PS as a function of temperature, molecular weight, and concentration which would allow us to construct a family of isoviscous state curves as was done in Figure 17 of ref 9 for pure PS. As is well-known, zero-shear melt viscosity, η_0, shifts from a first-power to a 3.4-power dependence on M at M_c because of the onset of entanglement (see Figures 10 and 11, p 244, ref 8). We assume that the ball bearing probe used to detect T_{gel} responds to the presence of entanglements by requiring a higher temperature to maintain isoviscous state conditions. This is a logical interpretation of the sudden increase in T_{gel} at M_c as seen in Figure 1. Experimental verification from moderately concentrated solution viscosity data is desirable.

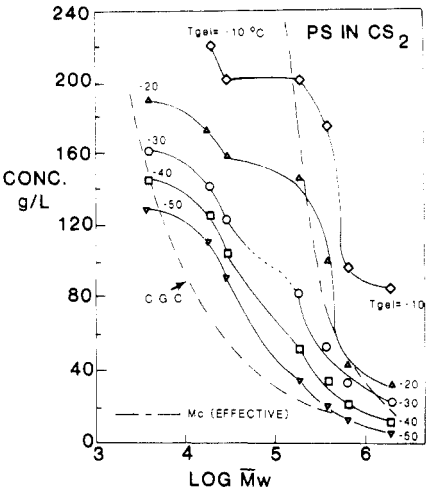

Figure 5. Plots of concentration (g/L) for PS in CS_2 against log $\bar{M}_w$ for the indicated iso-T_{gel} conditions. Behavior in regimes II and III is thus delineated.

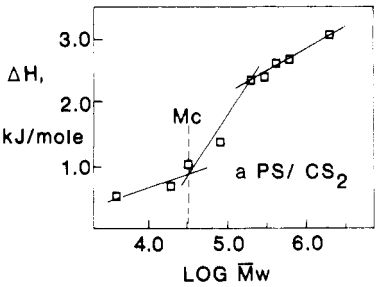

Figure 6. Interpretation of enthalpies of activation, ΔH, from Figure 11 of ref 3 as being influenced by entanglement effects. Data for PS in CS_2.

Table IV
Dependence of T_{gel} on Solubility Parameter, $\delta^{1/2}$, at 150 g/L and $\bar{M}_w = 6.7 \times 10^5$

no.	solvent	$\delta_s^{1/2}$ [a]	T_{gel}, [b,d] °C	$(\delta_p^{1/2} - \delta_s^{1/2})^2$	swelling ratio[c]
1	*n*-amyl acetate	7.8	−58	1.69	4.53
2	isoamyl acetate	8.5	−60	0.36	
3	1-chloropropane	8.1	−85	1.21	
4	1-chlorobutane	8.1	−84	1.21	
5	1-chloropentane	8.3	−81	0.64	
6	*n*-butyl acetate	8.5	−70	0.36	
7	*n*-propyl acetate	8.8	−70	0.09	
8	toluene	8.9	−96	0.04	20.7
9	THF	9.1	−108	0	21.0
10	CS_2	10	+10	0.81	
11	none	9.1			

[a] Table II of ref 3. [b] Estimated from Figures 6 and 7 of ref 3 at 150 g/L. [c] Volume swelling ratio for lightly cross-linked PS gels; data from ref 12. [d] Values of T_{gel} are increased by chain entanglement, presumably to about the same extent.

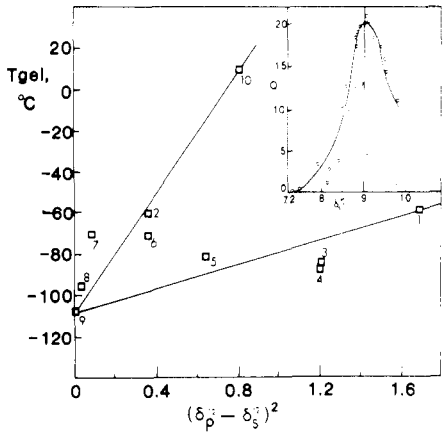

Figure 7. Correlation of T_{gel} at 160 g/L with $(\delta_p^{1/2} - \delta_s^{1/2})^2$, where $\delta_p^{1/2}$ and $\delta_s^{1/2}$ are solubility parameters for polymer and solvent, respectively. The upper line is considered normal; the bottom one may result from specific polymer–solvent interaction. Numbers identify diluents in Table IV. $\bar{M}_w = 6.7 \times 10^5$; hence entanglements are increasing T_{gel}. Inset shows swelling ratio, Q, vs. $\delta_s^{1/2}$ for styrene–divinylbenzene copolymers from ref 12.

Influence of Solvent on T_{gel}

Values of T_{gel} at C = 150 g/L were estimated from enlargements of Figures 6 and 7 of ref 3 and are collected in Table IV. These refer to constant $\bar{M}_w$ = 670 000. This concentration was arbitrarily chosen because it crossed the largest number of curves in these two figures. When T_{gel} at this fixed concentration is plotted against the solubility parameter of the solvent, $\delta_s^{1/2}$, also listed in Table IV, a U-shaped curve results with the minimum occurring when $\delta_s^{1/2} = \delta_p^{1/2}$, where $\delta_p^{1/2}$ is the solubility parameter of PS. However, there is scatter on the left-hand branch suggestive of specific solvent–polymer effects.

It is known from the pioneering work of Gee that swelling of lightly vulcanized rubber at fixed temperature is a maximum in solvents having the same $\delta^{1/2}$ as does the polymer.[11] Boyer and Spencer[12] showed similar results for lightly cross-linked styrene–divinylbenzene copolymers. Equilibrium volume swelling ratios from ref 12 for three of the diluents used are added to the last column of Table IV. It was also apparent from ref 12 that there were several families of solvents which reacted in different manners with the styrene–DVB copolymer.

T_{gel} values in Table IV offer another manifestation of this general effect in a reverse fashion by showing a minimum in T_{gel} when $\delta_p^{1/2} = \delta_s^{1/2}$. At the same time, evidence for several families of solvents was present. This latter effect becomes more evident in a plot of T_{gel} against $(\delta_p^{1/2} - \delta_s^{1/2})^2$ in which two straight lines appear. This is seen in Figure 7, whose inset depicts the swelling data from ref 12.

These solubility results suggest that the reversible thermal gelation behavior is related to a segment–segment interaction which is hindered by very good solvents such as toluene and tetrahydrofuran and promoted by a poor solvent such as CS_2. This segment–segment interaction will be discussed later.

It will be noted that there are no data points for $\delta_s^{1/2}$ lying between that of THF and CS_2. Such solvents are listed in Table II of ref 3 but did not form gels because freezing intervened before gelation could occur.

In addition to the solubility parameter effect, there is an influence of solvent molecular weight, M_s, as already noted in ref 3. T_{gel} at 160 g/L increases linearly with M_s, with the marked exception of CS_2. This is a well-known effect with T_g in that the ability of a diluent to suppress T_g decreases linearly with M_s, albeit with scatter. Such an effect was predicted by Kanig's free volume theory of T_g.[13] CS_2 (T_{gel} = 10 °C) and THF (T_{gel} = −108 °C) have almost identical values of M_s and thus dramatize the importance of $\delta_s^{1/2}$.

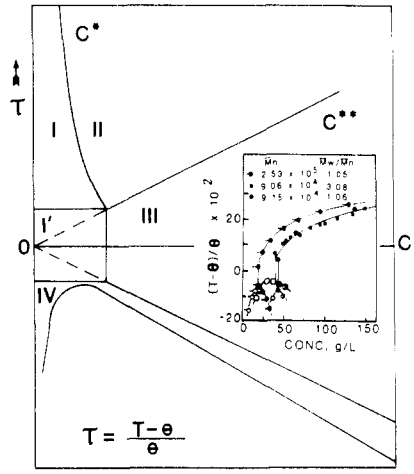

Figure 8. Phase diagram of a polymer solution from Daoud and Jannink.[14] The inset shows typical behavior of the aPS/CS_2 system.[3] The solid points indicate the sol–gel transition while the coexistence region is defined by open (two-phase solution) or half-filled (two-phase gel) points.

In general, those solvents with $\delta_s^{1/2} \ll \delta_p^{1/2}$ for which T_{gel} is lower than one would predict from $\delta_s^{1/2}$ using the upper (normal) branch of Figure 7 tend to have a polar group on one end and a hydrocarbon on the other. *n*-Amyl acetate is such an example. One may speculate that these molecules associate at low temperature so that the effective $\delta_s^{1/2} > \delta_p^{1/2}$. The $\delta_s^{1/2}$ values are obtained at normal temperatures where such association would be minimal. Doubling of molecular weight by association would have a contrary effect.

Phase Diagram

A typical phase diagram of PS in CS_2 exhibits qualitatively certain important features predicted by Daoud and Jannink[14] in the temperature–concentration diagram of polymer solutions. In particular, a predicted crossover in the semidilute region from critical to tricritical behavior coincides approximately with the sol–gel transition curve. The theory suggests a smooth change of behavior in the vicinity of the θ point from repulsive to attractive interaction. We suggest that in certain cases the change is not smooth but is manifest as a change in physical state, specifically gelation.

The phase diagram in the (τ, C) plane, where τ is the reduced temperature $(T - \Theta)/\Theta$, of Daoud and Jannink is shown in Figure 8. Below the Θ temperature the coexistence lines define a sharp transition. Above the Θ temperature a smooth change in behavior is indicated in the C^* lines separating the dilute (I and I') and semidilute (II and III) regions. A set of lines in the semidilute region indicates a change from repulsive (II) to attractive (III) interaction. The C^{**} line is assumed to be a smooth transition, and while Daoud and Jannink do not discuss the implications of the C^{**} line in terms of solution structure, it is reasonable to suppose that it marks the change from contacting to interpenetrating spheres.

A typical temperature–concentration diagram of polystyrene in CS_2 obtained by Tan et al.[3] is included as an inset in Figure 8. The various regions of the two-phase diagrams compare as follows:

(a) C^* Transition. The C^* transition is smooth but we think one point is observed in the gelation diagram at the critical gelation concentration (CGC) which defines the

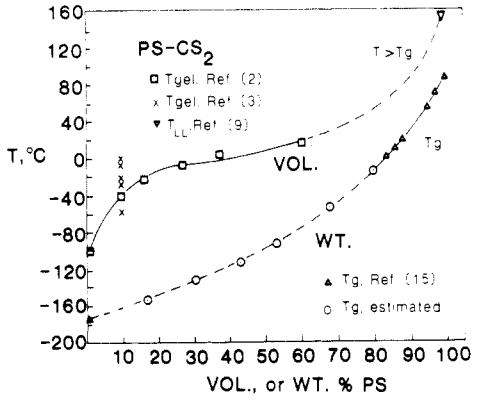

Figure 9. Comparison of T_{gel}, PS in CS_2 (upper curve from ref 2), with T_g values measured above $w_2 = 0.8$ from ref 15; calculated from $0 < w_2 < 0.8$. T_g for CS_2 from ref 15, $T > T_g$ for PS from ref 9. Crosses at $w_2 = 0.10$ are estimated from Figure 4 of ref 3 with $\bar{M}_w$ from bottom to top increasing from 2×10^4 to 2×10^6.

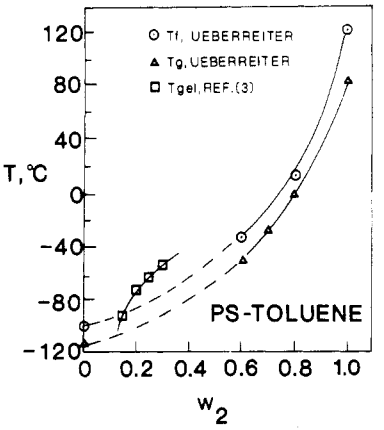

Figure 10. Comparison of the high-concentration penetrometer data of Ueberreiter for PS–toluene showing T_g and $T_f > T_g$ values with moderate-concentration T_{gel} values from ref 3. Values of T_{gel} for $w_2 = 0.2$–0.3 appear clearly above T_g but approach T_g at lower concentration. w_2 is the weight fraction of PS.

lowest concentration at which a gel can be obtained. The CGC has the correct dependence of C^* on the inverse square root of the degree of polymerization. It is reasonable to identify the CGC with the intersection point of regions I, I′, II, and III. The vertical straight line obtained by connecting the CGC to the coexistence curve then identifies the crossover region I′ to region III.

(b) C^{**} Transition. We suggest that the coincidence of the sol–gel curve and the C^{**} line is not fortuitous. The correspondence is remarkable even though comparison in detail reveals certain inconsistencies. Specifically, the predictions that the C^{**} line is linear and independent of molecular weight are not confirmed by the experiments. The experimental sol–gel curve is better described by the van't Hoff relationship and shifts significantly to lower temperatures as the molecular weight is decreased. It is essential to note here that not all solvents form gels with polystyrene, while others form gels only well below the C^{**} line. The implication is that interpenetration of the coils is necessary for gelation but an additional factor which stabilizes the contacts between chains is also required.

Distinction between T_{gel} and T_g

It was stated in ref 3 (bottom right-hand column, p 31) that "gel formation does not appear to be synonymous with the glass transition of highly plasticized polymer". Reference was then made to measurement of T_g by Jenckel and Heusch, using the refractive index method, on the system PS–CS_2.[15] This conclusion has now been confirmed by a variety of studies to be discussed.

Jenckel and Heusch[15] presented tabulated values of T_g from $w_2 = 0.838$–1.000, where w_2 is the weight fraction of PS in CS_2. They gave without elaboration a T_g of −175 °C for CS_2. These data were linearized by us using the Gordon–Taylor copolymer equation[16] in the form employed by Wood.[17] This linear plot permitted estimation of T_g values in the composition interval from $w_2 = 0$ to $w_2 = 0.832$. T_{gel} values from 0.10 to 0.66 volume fraction PS ($\bar{M}_n = 37\,000$)CS_2 were estimated from Figure 1 of ref 2. Ignoring the difference between weight and volume fraction, we compare in Figure 9 the T_{gel} values of ref 2 with the T_g values from ref 15. This plot leaves no doubt about a clear distinction between T_{gel} and T_g. It is not clear why the difference $T_{gel} - T_g$ is so large unless T_g for pure CS_2 is in error. Since the highest concentration for T_{gel} is close to the lowest concentration for T_g, any doubts about the distinction are minimized. The point on the upper curve for pure PS is also for $\bar{M}_n = 37\,000$ but obtained by both DSC and torsional braid analysis from ref 9. It is a $T >$ T_g event. There is no reliable value of molecular weight for the ref 15 PS but we believe from the T_g value that it is a commercial PS containing oligomers, with a probable $\bar{M}_n \sim 10^5$.[18]

It is clear that the T_{gel} values of Figure 9 are not distorted by entanglement effects and represent the regime II overlap mechanism of Figure 4. It is naturally desirable to locate other examples showing a distinction between T_{gel} and T_g, and for this we examine the $T_f > T_g$ phenomena of Ueberreiter[19] as well as T_{ll} data by Gillham and coworkers[21] and by Colborne.[22]

$T > T_g$ Phenomena in Other PS–Diluent Systems

Ueberreiter[19] has studied a number of PS–diluent systems by the method of penetrometry. In all cases he observes both T_g and $T_f > T_g$ as a function of polymer concentration expressed as a weight fraction. A molecular weight is not stated for the PS used. Since its $T_g = 85$ °C, we can assume that it was most likely a commercial PS, $\bar{M}_n \geq 10^5$, containing monomer, dimers, and trimers which lowered T_g from the normal 100 °C to the value given.[18]

In the case of simple diluents he covered the composition range from $w_2 \sim 0.5$ to $w_2 = 1.0$. Toluene and methyl isobutyl ketone are two such diluents employed. By estimating T_f and T_g from Figure 8 of ref 19, using a known T_g for toluene of −114 °C,[20] and assuming a T_f for toluene, we prepared the plot shown in Figure 10. Superimposed are values of T_{gel} for PS, $\bar{M}_w = 6.7 \times 10^5$, in toluene. Such comparisons must be considered with caution because of the widely different techniques and the closeness of the two sets of temperatures. Penetrometry involves motion of a weighted probe at unspecified shear rate, while the ball bearing of ref 3 is presumably acting at or near zero-shear conditions. But it does appear as if T_{gel} at the higher concentrations such as 300 g/L is more closely related to T_f than to T_g whereas at the lower concentrations, i.e., 150 g/L, T_{gel} is approaching the T_g curve. The assumption of $T_f \sim -100$ °C for toluene is based on Figure 8 of ref 19 showing that $T_f - T_g \rightarrow 15$ K at $w_2 = 0.5$.

Ueberreiter also determined T_f–w_2 values for plasticizer–PS systems for which measurements were possible from $w_2 = 0$ to $w_2 = 1$. Gillham et al.[21] measured both T_g and a $T > T_g$ phenomenon labeled T_{ll} by torsional braid analysis over the entire composition range on a PS of $\bar{M}_n = 37\,000$ (hence no entanglements). Colborne[22] used a falling ball method to measure melt viscosity of plasticizer–PS systems in the composition range $w_2 = 0.085$–0.50. He estimated a $T > T_g$ event both from the viscosity data

and from tack temperatures. He compared his $T > T_g$ values with T_g from the literature for the same PS–plasticizer systems.

These various examples from the prior literature[19,21,22] consistently demonstrate the existence of a transition or relaxation lying above T_g in PS–diluent systems. This fact lends credence to our conclusion that T_{gel} is not only greater than but different from T_g for each of the various PS–diluent systems studied.[2,3]

This conclusion gains additional support by considering the K_{gel} values collected in Table II. K_{gel} from T_{gel} data at C = 140 g/L, from T_f values on PS (1040 g/L), and from T_{ll} for PS (again at 1040 g/L) are almost identical. K_{gel} then climbs abruptly at lower concentrations, indicating that T_{gel} is approaching a dilute solution type of behavior, possibly moving from regime II to regime I of Figure 4 or from region II to region I of Figure 8.

Differential Scanning Calorimetry (DSC)

Prior to locating the Ueberreiter data on PS–diluent systems,[19] we carried out some exploratory experiments with an anionically prepared PS (mostly $\bar{M}_n$ = 37 000) with several diluents at w_2 = 0.40–1.0 A Du Pont 990-910 DSC was employed, using sealed DSC pans. Diluents included CS_2, toluene, decalin, and n-butyl acetate. Heating rate was 10 K min^{-1}, and sensitivity setting was 0.1 mJ s^{-1} cm^{-1}.

Results tended to be erratic because of one or more of the following factors: small samples required, low concentrations of diluent, loss of volatiles during preparation, improper mixing and decreasing intensity of the transitions.

Several consistent observations emerged:

(a) There were always two events on the DSC trace: an endothermic step at T_g and an endothermic slope change at $T > T_g$.

(b) Both moved to lower temperature as w_2 decreases.

(c) The ratio $(T > T_g)/T_g$ ranged from 1.12 to 1.25, with an average of 1.18. This ratio was lower in general the lower was T_g, consistent with the observations of Ueberreiter[19] about $(T > T_g) \rightarrow T_g$.

DSC studies were discontinued in view of the systematic data already in the literature.[19,21,22] DSC remains an alternate technique still requiring refinements in procedure. See also the DSC evidence for T_{gel} in Figure 8 of ref 3.

Mechanisms for Reversible Gel Formation in Atactic PS Solutions

General conditions for three-dimensional gel formation are given in the Introduction of ref 3. It was recognized that there is no unequivocal explanation for irreversible gel formation of the type reported in ref 3 for atactic PS.

Gel formation was treated in ref 3 using the Ferry–Eldridge relationship[23]

$$\ln C = \text{constant} + \Delta H_m/RT_m \qquad (5)$$

developed for gels formed from solutions of crystallizable polymers. C is concentration, ΔH_m is the heat absorbed to form a mole of junction points, and T_m is the melting point, which is taken in our case as T_{gel}. The validity of this approach was demonstrated in Figure 10 of ref 3. The calculated values of ΔH_m for atactic PS were less than those for crystallizable polymers. Evidence for the existence of short helical 3_1 sequences in atactic PS has been reviewed in ref 1. Such moieties may possibly play a role in the gelation process. However, the complete thermal reversibility of the atactic PS gels argues against the existence of crystallizable elements, however short. Known low levels of crystallinity can influence gelation, as we have demonstrated in a companion study.[24] In the most general case, one needs a mechanism that does not rely on borderline crystallinity in so-called atactic polymers.

Frenkel and his colleagues have recently proposed a phase dualism mechanism to account for the existence of a $T > T_g$ transition in amorphous polymers and polymer–diluent systems.[25,26] The basic assumption is that segments of a macromolecule engage in liquid-like contacts with other segments in the same or neighboring chains. Opposing this is a gain in entropy by the macromolecule as it is freed of such local restraints at elevated temperature, specifically at $T > T_g$. They employ the term "segmental melting" (p 1160 of ref 25) but do not suggest an implied formalism such as $T > T_g \cong \Delta H_m/\Delta S$. They were discussing the T_{ll} transition (relaxation) in bulk polymers. However, as discussed in ref 26, Baranov and Frenkel recognized that the presence of diluents would depress this "segmental melting" temperature. They further recognized that segment–segment interaction would be enhanced by chain stiffness and by polarity.

As noted in ref 26, such segment–segment contacts in an amorphous polymer in the liquid polymer regime, $T_g < T < T_{ll}$, would give rise to a three-dimensional network which would "melt out" at T_{ll}. This effect appears to be a necessary and sufficient condition for reversible gelation at $M < M_c$(eff).

Recently reported studies of Clark et al.[28] using dynamic rheological measurements clearly show that the viscoelastic properties of polystyrene in CS_2 change dramatically at the gel point with a value of G' independent of the frequency and of a magnitude appropriate to a classical three-dimensional network. The frequency dependence of G' and G'' and the rapid approach to equilibrium values lead them to conclude that "neither chain entanglements nor microcrystallite formation explains the interchain interaction." Additional results not included in ref 28 but presented in the poster session at the Aug 1983 ACS Meeting in Washington, DC, demonstrate that the gel is destroyed under steady shear but re-forms immediately with normal values of G' and G'' when the shear field is removed. Reversibility of gelation to application and removal of a shear field is totally consistent with complete thermal reversibility and is predictable by the segment–segment interaction mechanism discussed above.

Associated with this segment–segment local melting is an implied ΔH_m not unlike that in eq 5 for crystallizable systems. ΔH_m should depend on the solvent and polymer characteristics such as chain stiffness and polarity. ΔH_m should depend only slightly on $\bar{M}_w$, in contrast to the behavior shown in Figure 6. Figure 6 is based on a macroscopic viscosity measured by the ball bearing and must reflect entanglements. Precision calorimetry should give a true ΔH_m uninfluenced by entanglements. Figure 8 of ref 3 is a DSC trace indicating an endothermic peak which might well reflect a correct value of ΔH_m.

The Lobanov–Frenkel phase dualism hypothesis[25,26] appears to provide a molecular level mechanism whereby a thermally reversible gel can form in any atactic polymer–diluent system. While their paper discusses T_{ll}, it is not necessary to invoke the T_{ll} symbolism in the present case. T_{gel} is a precise designation for the observed phenomena with atactic PS in a variety of diluents. T_{gel} is a $T > T_g$ process such as Lobanov and Frenkel were discussing.

Ueberreiter introduced the terminoloty T_f to express his belief that there should be a molecular weight dependent $T > T_g$ transition at which intramolecular barriers to rotation about the backbone chain are overcome.[29] It was his view that the polymer melt in the temperature region

$T_g < T < T_f$ was a "fixed liquid", i.e., one possessing some unspecified structure. The true liquid state prevailed only at $T > T_f$. His first experimental determination of T_f appeared in ref 4. His early perception of the nature of polymer melts is quite consistent with the modern views of Frenkel and co-workers.

We might return briefly to the mixed isotactic PS–atactic PS–diluent effects from ref 1 mentioned in the Introduction. Since the atactic PS was present at 16% concentration, it was capable of forming a gel at sufficiently low temperature. It seems plausible that it could incorporate isotactic chains into that network through simple isotactic segment–atactic segment contacts. Pursuit of such mixed isotactic–atactic systems could well provide further insights into the behavior of purely atactic PS–diluent systems, as predicted in ref 1.

Summary and Conclusions

1. We confirm an earlier conclusion[3] that overlap of macromolecules is a necessary and sufficient condition for gel formation in atactic PS–diluent systems.

2. Physical entanglements present at higher molecular weights and higher concentrations enhance gel stability as manifested by persistence of gels to higher temperature for any given M_w–diluent pair.

3. Three distinct regimes in the sol–gel behavior have been identified. Regime I covers nongelling solutions: regime II is gelation with overlap but without entanglements; regime III is gelation stabilized by entanglements.

4. Critical entanglement molecular weights, M_c(eff) follow the relationship

$$M_c(\text{eff})v_2 = \text{constant}$$

where v_2 is the volume fraction of polymer (for convenience we use weight fraction) and/or concentration in g/L, which changes the value of the constant.

5. At fixed concentration (160 g/L) T_{gel} passes through a minimum as the interaction parameter of the solvent, $\delta_s^{1/2}$, approaches that of PS, $\delta_p^{1/2}$. In addition, there are specific solvent–polymer interaction effects.

6. Thermodynamics of dilute solution gels are further analyzed in terms of the Daoud–Jannink concepts of dilute solution behavior.

7. T_{gel} phenomena from ref 2 and 3 are compared with fusion-flow data of ref 4 for PS, the penetrometry data of ref 19 for various PS–diluent systems, the falling ball viscosity data of Colborne[22] for PS–diluent systems, and the T_{ll} results of Gillham et al. for PS[9] and PS–diluent systems.[21] Such comparisons demonstrate the existence of two events, T_g and $T > T_g$. We cannot state unequivocally that T_{gel} is the same as the T_f of Ueberreiter or the T_{ll} of Gillham[21] and Colborne[22] but they appear to be related.

8. We show conclusively for PS–CS_2 and tentatively for PS–toluene that T_{gel} is different from and greater than T_g except perhaps at the lowest concentration of PS in diluent. We confirm a conclusion suggested in ref 3 that T_{gel} is not a T_g phenomenon.

9. The segment–segment interaction mechanism of Lobanov and Frenkel provides a plausible molecular level interpretation of thermally reversible gelation in atactic polymers, with T_{gel} representing the temperature of "segmental melting". This is consistent with the solubility parameter data of Figure 7 and the sharpness of the T_{gel} melting process.

10. Conversely, T_{gel} data may provide the best and most comprehensive experimental evidence yet available for the segment–segment "local melting" mechanism of Frenkel et al.[25,26]

11. T_{gel} phenomena should be a characteristic feature of all atactic polymers.

12. Destruction of atactic PS gels at fixed temperatures by application of a shear field and re-formation of the gel on removal of the shear are consistent with the segment–segment interaction mechanism postulated herein to explain gelation.

Acknowledgment. It has been our privilege to discuss the concepts in this paper on several occasions with Professor Andrew Keller (University of Bristol) and to modify the paper in response to his views. We do not wish to infer that Professor Keller endorses any or all of the concepts which we have advanced. We are indebted to Kathleen M. Panichella for exploratory DSC experiments on PS–diluent systems at polymer concentrations of $w_2 = 0.6$–1.0 and for the line drawings, and to Susan Haywood of MMI for the electronic typing.

Registry No. PS (homopolymer), 9003-53-6.

References and Notes

(1) Girolamo, M.; Keller, A.; Miyasaka, K.; Overbergh, N. *J. Polym. Sci., Polym. Phys. Ed.* **1976**, *14*, 39.
(2) Wellinghoff, S.; Shaw, J.; Baer, E. *Macromolecules* **1979**, *12*, 932.
(3) Tan, H.-M.; Moet, A.; Hiltner, A.; Baer, E. *Macromolecules* **1983**, *16*, 28.
(4) Ueberreiter, K.; Orthmann, H.-J. *Kunststoffe* **1958**, *48*, 525.
(5) Bueche, F. *J. Appl. Phys.* **1953**, *24*, 423.
(6) Bueche, F. *J. Appl. Phys.* **1955**, *26*, 738.
(7) Fox, T. G.; Loshaek, S. *J. Appl. Phys.* **1955**, *26*, 1080.
(8) Ferry, J. D. "Viscoelastic Properties of Polymers", 3rd ed.; Wiley: New York, 1980; p 504.
(9) Stadnicki, S. J.; Gillham, J. K.; Boyer, R. F. *J. Appl. Polym. Sci.* **1976**, *20*, 1245.
(10) Turner, D. A. *Polymer* **1978**, *19*, 789.
(11) Gee, G. *Trans. Faraday. Soc.* **1942**, *38*, 418; *Trans., Inst. Rubber Ind.* **1943**, *18*, 266.
(12) Boyer, R. F.; Spencer, R. S. *J. Polym. Sci.* **1948**, *3*, 97.
(13) Kanig, G. *Kolloid Z. Z. Polym.* **1963**, *190*, 1; **1965**, *20*, (3) 161.
(14) Daoud, M.; Jannink, G. *J. Phys. (Paris)* **1976**, *37*, 973.
(15) Jenckel, E.; Heusch, R. *Kolloid Z.* **1953**, *130*, 89. An enlarged plot of these T_g data is given by Ferry, Figure 17.1, p 488, of ref 8.
(16) Gordon, M.; Taylor, J. S. *J. Appl. Chem.* **1952**, *2*, 493.
(17) Wood, L. A. *J. Polym. Sci.* **1958**, *28*, 219.
(18) Boyer, R. F., personal experience.
(19) Ueberreiter, K. In *Adv. Chem. Ser.* **1965**, *No. 48*, 35ff.
(20) Carpenter, M. R.; Davies, D. B.; Matheson, A. J. *J. Chem. Phys.* **1967**, *46*, 2451.
(21) Gillham, J. K.; Benci, J.; Boyer, R. F. *Polym. Eng. Sci.* **1976**, *16*, 357.
(22) Colborne, R. S. *J. Macromol. Sci., Phys.* **1967**, *B1*, 517.
(23) Eldridge, J. E.; Ferry, J. D. *J. Phys. Chem.* **1954**, *58*, 992.
(24) Tan, H.-M.; Chang, B. H.; Baer, E.; Hiltner, A., *Eur. Polym. J.* **1983**, *19*, 1021.
(25) Lobanov, A. M.; Frenkel, S. Ya. *Polym. Sci. USSR (Engl. Transl.)* **1980**, *22*, 1150 (original in *Vysokomol. Soedin., Ser. A* **1980**, *22*, 1045).
(26) See discussion of Frenkel–Baranov phase dualism mechanism on p 540–542 of ref 27.
(27) Boyer, R. F. *J. Macromol. Sci., Phys.* **1980**, *B18*, 461.
(28) Clark, J.; Wellinghoff, S. T.; Miller, W. G. *Polym. Prepr., Am. Chem. Soc., Div. Polym. Chem.* **1983**, *24* (2), 86.
(29) Ueberreiter, K. *Kolloid Z.* **1943**, *102*, 272, especially Figure 10.